

Vortex based seedingless image velocimetry using high-speed holography

Johannes Gürtler^{1*}, Felix Greiffenhagen², Jakob Woisetschläger²,
Jürgen Czarske¹

¹TU Dresden, Laboratory for Measurement and Sensor System Techniques, Dresden, Germany

²TU Graz, Institute of Thermal Turbomachinery and Machine Dynamics, Graz, Austria

* johannes.guertler@tu-dresden.de

Abstract

Investigations of complex flow phenomena require simultaneous detection and correlation of several quantities, e.g. density and velocity inside a reactive flow where the addition of seeding particles can disturb the chemical reaction. We present a high-speed camera-based interferometric system which enables simultaneous seedingless measurement of density fluctuations and velocity inside a turbulent flow. This new measurement approach is based on correlation of vortex movement, which is now detectable due to the development of high-speed cameras, enabling imaging with high spatial resolution of 0.47 mm^2 and pixel wise signal processing at a high frame rate of 200 kHz. The progress for research is an additional tool for flow measurements without drawbacks like particle slippage or disturbance of fluid properties like density or temperature.

1 Introduction

Environmental protection and sustainability are the focus of current research, such as in the areas of aero-engines for civil aviation or power generation. Technological progress in those fields is based on an improved knowledge of physical principles, which is gained by continuous developments in optical metrology, like digital holography for density or vibration measurements (Lagny et al. (2018)), particle based flow measurement techniques (Gürtler et al. (2016), Gürtler et al. (2017), Scharnowski et al. (2019)) or spectroscopic approaches for the investigation of reaction processes (Greiffenhagen et al. (2019)). Simultaneous detection and correlation of several quantities or 3D imaging and solution of the inverse problem are necessary in order to understand complex physical phenomena. However, application of several measurement systems at the same time is not always possible due to limitations like optical access or mutual disturbance of the systems, e.g. seeding particles inside a reactive flow.

We demonstrate simultaneous fluid density and seedingless flow measurements using high-speed camera-based digital holography and image correlation. The measurement approach is based on the interferometric detection of density fluctuations up to 30 kHz inside a non-stationary flow, where vortex structures move with the main flow. The velocity of the vortices is then determined by image correlation techniques. This new combined detection without the usage of seeding particles enables the development of enhanced system modelling for turbulent flows and improved technological application. The measurement system offers high data rates of 2 GByte/s based on the used high-speed camera. As an example the fluctuating heat release rate and vortex velocity inside of a swirl-stabilized flame are measured by evaluating spatio-temporal optical density fluctuations.

2 Principle and Setup

The experimental setup is a high-speed camera based Mach-Zehnder interferometer as depicted in Fig. 1, using a *Cobolt Samba* as light source. The measurement beam is expanded to a field of view of $47 \times 47 \text{ mm}^2$.

After passing the measurement volume, the laser light is imaged through a telecentric lens setup on a *Phantom v1610* high-speed camera running at 200 kHz using 100x100 px, resulting in a spatial resolution of 0.47x0.47 mm². At every pixel the interferometric intensity signal with the phase shift

$$\Delta\phi = 2\pi f_B t + \frac{2\pi}{\lambda} L \quad (1)$$

is detected, with the laser wavelength $\lambda = 532$ nm, the carrier frequency $f_B = 50$ kHz and the length of the optical path

$$L = \int n dz \quad (2)$$

with the refractive index n , which is linear depending on the fluids density ρ , according to the Gladstone-Dale relation

$$G = \frac{n-1}{\rho} \quad (3)$$

with the fluid dependent Gladstone-Dale constant G . Based on the instantaneous frequency

$$f_I = \frac{\partial \Delta\phi}{2\pi \partial t} = f_B + \frac{\dot{L}}{\lambda} = f_B - f_D \quad (4)$$

of the intensity signal it is possible to detect temporal density fluctuations $\dot{\rho}$ integral along the laser beam in z -direction. This instantaneous frequency is determined for each time step of the camera intensity signal using the Hilbert transform and quadrature demodulation. The density fluctuation is then calculated using eq. (2)-(4).

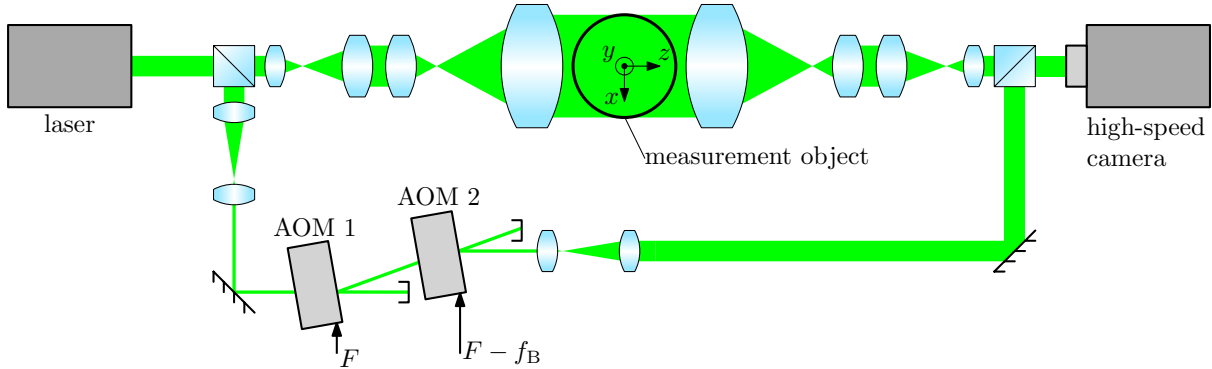


Figure 1: Schematic Mach-Zehnder setup. The laser with wavelength $\lambda = 532$ nm is expanded to a measurement volume of 47x47 mm² in the $x-y$ -plane. The measurement object is centered in the shown coordinate system and the reference beam is frequency modulated with $f_B = 50$ kHz using two acousto optic modulators (AOM). The interferometric signal is detected on a *Phantom v1610* high-speed camera with a frame rate of 200 kHz at 100x100 px.

As example experiment, the fluctuating density inside a swirl-stabilized flame is measured. The used burner is described in more detail by Schlüßler et al. (2015). It is fueled by a premixed propane-air-flow, which is swirled by four tangential inlets of a bushing inside the burner. The ring shaped burner outlet has a diameter of 15 mm and a variable cross section which was adjusted to 2 mm. Within the flame volume, the density fluctuation depends on local fluctuations of the heat release rate \dot{q} within an infinitesimal volume according to

$$\dot{\rho} = \frac{\kappa-1}{c^2} \dot{q} \quad (5)$$

with the sound velocity c and the temperature dependent adiabatic exponent κ (Dowling and Morgans (2005), Greiffenhagen et al. (2019)). Thus, the frequency shift

$$f_D = \frac{G(\kappa-1)}{\lambda c^2} \int \dot{q} dz = \frac{G(\kappa-1)}{\lambda c^2} \dot{Q}. \quad (6)$$

is linear depending on the integral heat release rate \dot{Q} along the laser beam, crossing the flame volume in its entirety (cf. Greiffenhagen et al. (2019)). Along this line-of-sight the heat release rate of the flame can oscillate with a dominant resonance frequency and a turbulent fluctuation, both depending on the chosen working point of the burner, adjusted via the controlled mass flow of propane and air, respectively. The spatial distribution of the resonant oscillating part of the heat release rate is approximately rotational symmetric around the z -axis and, thus, local data can be calculated from the phase averaged integral data using inverse Abel transform. By this procedure the spatio-temporal distribution of vortex like density structures is revealed. Finally, the movement of those structures is determined based on image correlation.

3 Results

3.1 System Validation

In order to validate the camera-based system, reference measurements were performed, comparing the new system to an industrial standard pointwise vibrometer from the manufacturer *Polytec*. Both systems were used simultaneously to measure the density fluctuation inside a swirl-stabilized flame, adjusted to a resonance frequency of 213 Hz. The *Polytec* system uses a single photo detector and a collimated laser beam of 2 mm diameter. Therefore, the field of view of the CLIV system was reduced by using 6x6 px. Additionally, a Gaussian weighted averaging of the detected intensity was applied, before performing the signal processing described in section 2.

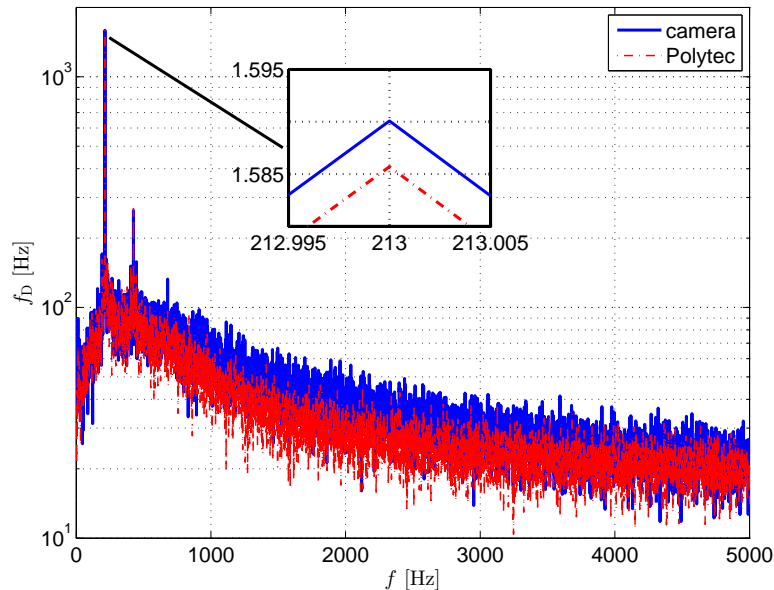


Figure 2: Reference measurements of the frequency shift f_D based on density fluctuations inside a swirl-stabilized flame. Comparison between industrial *Polytec* vibrometer and the high-speed camera-based system.

The amplitude spectrum of the detected frequency shift f_D is shown in Fig. 2, calculated from the complete signals with a measurement duration of 9 s, using a window length of 1 s. In order to characterize the system noise, the standard uncertainty for each frequency is calculated based on 9 samples each. The uncertainty values are then averaged within the range from 0 Hz to 15 kHz, resulting in $\sigma_{f_D} = 3.82$ Hz for the *Polytec* system and $\sigma_{f_D} = 4.41$ Hz for the camera-based system, respectively. Both systems are in good agreement within the uncertainty range also influenced by the reproducibility of the flame operation point, and detect the same narrow-band oscillation at 213 Hz and its first harmonic as well as the broad-band turbulent density fluctuation. As result, the camera-based system is considered validated and was applied for full field measurements at swirl-stabilized flames.

3.2 Flame Measurements

Full field measurements of density fluctuations inside a swirl-stabilized flame were performed using the burner setup described in section 2. The controlled mass flows were adjusted to 1.80 kg/h and 140 g/h for air and propane, respectively, resulting in a dominant oscillation of the density at $f_{\text{res}} = 680$ Hz. The heat release rate was calculated from the line of sight frequency data based on eq. (6), using a Gladstone-Dale constant $G = 2.6 \times 10^{-4} \text{ m}^2/\text{kg}$ and the adiabatic exponent $\kappa = 1.38$ due to the chosen mass flows. As a result, the line of sight amplitude of the resonant oscillation at f_{res} is shown in Fig. 3, based on a fast Fourier transform (FFT) of the complete signal of 27 s, using a window length of 1 s. The center of the burner outlet is positioned at $(0, 0, 0)$. Due to the assumption of a rotational symmetric distribution, data points at positions $x > 0$ are averaged with data points at $x < 0$.

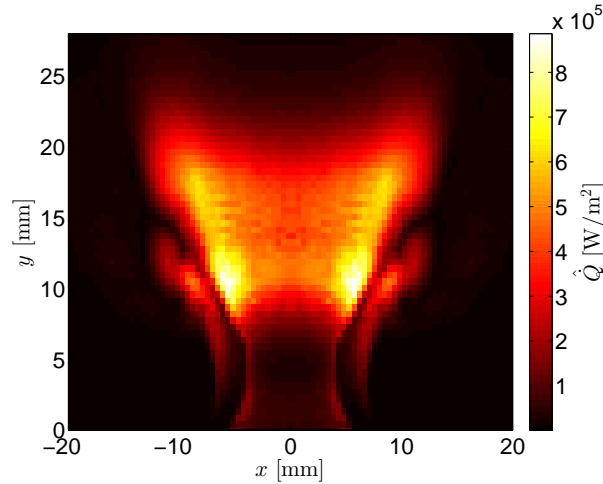


Figure 3: Line-of-sight amplitude of the heat release rate oscillation at $f_{\text{res}} = 680$ Hz, calculated from FFT of the 27 s signal, with a window length of 1 s.

In order to achieve local data of the heat release rate in the x - y -plane at $z = 0$, the measured line of sight data was phase averaged with f_{res} , resulting in 27×295 images, i.e. 678 time samples per image, before the inverse Abel transform was applied. In Fig. 4(a) and in Fig. 4(b), the phase averaged line-of-sight data and its inversion for one of those images is shown, respectively, after an additional spatio-temporal low pass filtering. Values in the area $0 \text{ mm} \leq x \leq 2 \text{ mm}$ were discarded due to artifacts from the inversion. As a result, local density clusters are revealed, which are moving upwards starting from the rim of the burner outlet, following the main gas flow.

Finally, the velocity of the detected density structures was calculated by image correlation using the open source PIV algorithm *PIVlab*. In Fig. 5(a) the detected mean value of the velocity is shown, based on averaging of all 7964 velocity fields. Values are discarded based on signal to noise ratio (SNR) of the image and interpolated afterwards using 3D spline interpolation. The normalized vector plot depicts the actual measurement points, resulting from the chosen size of 4 px of the last interrogation window (4 steps: 32, 16, 8, 4), i.e. a spatial resolution of 1 mm^2 . The color plot depicts the value of the vectors, using an additional grid interpolation of factor 2. As a comparison, velocity measurements at the same burner setup are shown in Fig. 5(b) based on Doppler global velocimetry with sinusoidal frequency modulation (FM-DGV) as described in Schlüßler et al. (2015) where seeding particles had to be added to the flow. The spatial resolution of FM-DGV was adjusted to 0.8 mm^2 and an averaging over 10 s, i.e. 1×10^6 samples was applied. Values were discarded based on low SNR due to the low amount of seeding particles outside the main flow.

The comparison of the two measurement results reveals a similar qualitative distribution of the velocity field, yet a strong difference of the actual values. At this point, it is not clear, whether the density structures follow the flow velocity of the gas or show a different movement, e.g. based on convection. However, the presented technique offers interesting opportunities due to the non-invasive detection of density variations in the field.

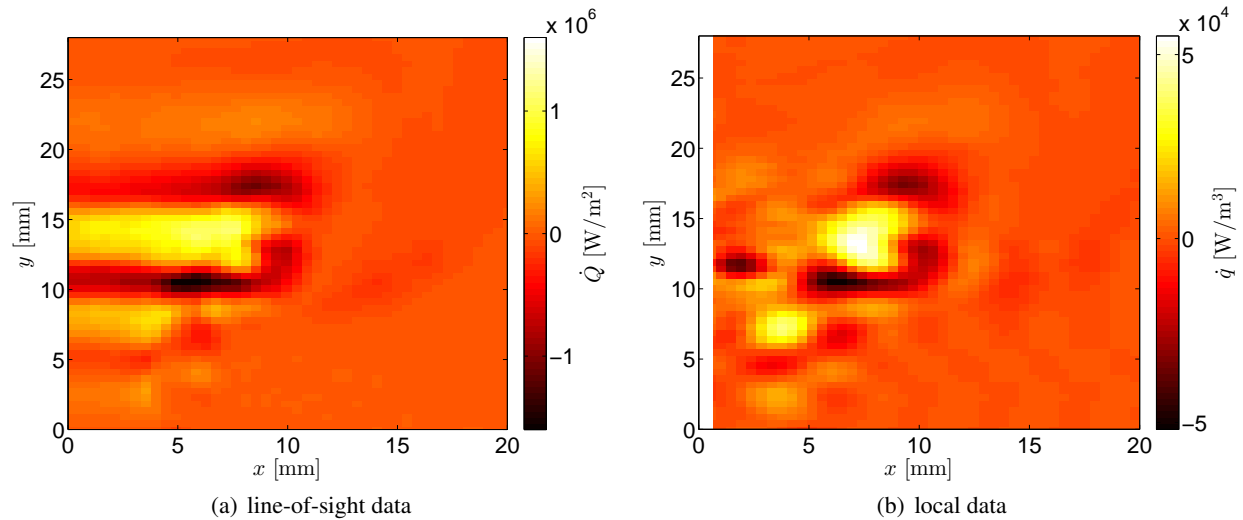


Figure 4: Measurement of the heat release rate inside a swirl stabilized flame, averaged for one phase step of the oscillation (phase averaged data) at $f_{\text{res}} = 680$ Hz. a) Line-of-sight data. b) Local heat release rate at position $z = 0$, calculated from line-of-sight data using inverse Abel transform.

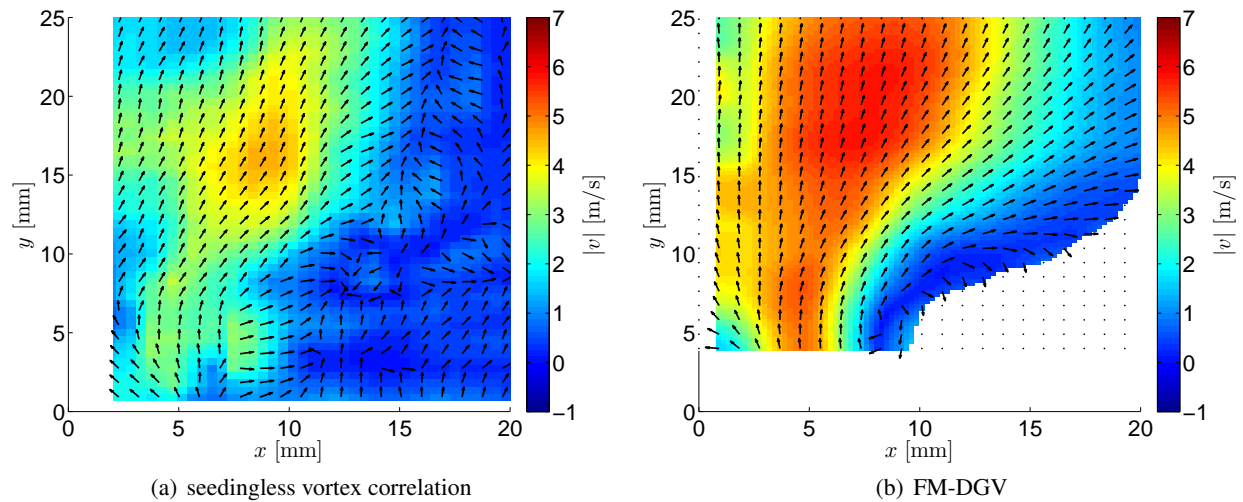


Figure 5: Velocity measurements inside a swirl-stabilized flame. The normalized vectors depict the actual measurement points, while the color plot depicts the value of the vectors using an additional grid interpolation. a) Velocity based on correlation of local density clusters and vortex structures. b) Velocity based on Doppler global velocimetry with sinusoidal frequency modulation (FM-DGV) as described in Schlüßler et al. (2015).

4 Conclusion

Simultaneous detection and correlation of several quantities like density and velocity of a turbulent gas flow is not always possible, e.g. due to the disturbance of chemical reactions when using particle based flow measurement techniques. Therefore, we presented a high-speed camera-based interferometric system with a high frame rate of 200 kHz at 100x100 px resolution. The new system enables the line of sight detection of density fluctuations up to 30 kHz inside a turbulent flow and the estimation of the velocity of local density structure based on image correlation. The detection of those local structures via inverse Abel transform was possible due to the rotational symmetric distribution of the density fluctuation.

In future experiments, the detection of 3D flow data based on tomographic reconstruction or a stereo approach is planned as well as further measurement applications like sound pressure variations at sound damping perforates of airplane engines.

Acknowledgements

The authors would like to thank ‘Deutsche Forschungsgesellschaft’ (DFG) and ‘Österreichischer Wissenschaftsfonds’ (FWF) for the financial support of the projects Cz55/33-1 and I2544-N30, respectively.

References

- Dowling AP and Morgans AS (2005) Feedback Control of Combustion Oscillations. *Annual Review of Fluid Mechanics* 37:151–182
- Greiffenhagen F, Peterleithner J, Woisetschläger J, Fischer A, Gürtler J, and Czarske J (2019) Discussion of laser interferometric vibrometry for the determination of heat release fluctuations in an unconfined swirl-stabilized flame. *Combustion and Flame* 201:315–327
- Gürtler J, Haufe D, Schulz A, Bake F, Enghardt L, Czarske J, and Fischer A (2016) High-speed camera-based measurement system for aeroacoustic investigations. *Journal of Sensors and Sensor Systems* 5
- Gürtler J, Schlüßler R, Fischer A, and Czarske J (2017) High-speed non-intrusive measurements of fuel velocity fields at high-pressure injectors. *Optics and Lasers in Engineering* 90:91–100
- Lagny L, Trujillo C, Le Meur J, Montresor S, Garcia-Sucerquia J, Heggarty K, Pezerat C, and Picart P (2018) Vibration retrieval from time sequences of digital on-line Fresnel holograms. *Imaging and Applied Optics* 2018 1:DM5F.2
- Scharnowski S, Bross M, and Kähler CJ (2019) Accurate turbulence level estimations using PIV / PTV. *Experiments in Fluids* 60:1–12
- Schlüßler R, Bermuske M, Czarske J, and Fischer A (2015) Simultaneous three-component velocity measurements in a swirl-stabilized flame. *Experiments in Fluids* 56:1–13